Studies on the Sulfur Poisoning of Ru–RuO$_x$/TiO$_2$ Catalyst for the Adsorption and Methanation of Carbon Monoxide

V. S. Kamble,* V. P. Londhe,* N. M. Gupta,[1,]* K. Ravindranathan Thampi,† and M. Grätzel†

*Chemistry Division, Bhabha Atomic Research Centre, Trombay, Bombay-400 085, India; and †Department of Chemistry, Swiss Federal Institute of Technology, Lausanne, CH 1015, Switzerland

The effects of sulfur poisoning on the chemisorption and on the methanation of carbon monoxide over Ru/TiO$_2$ catalyst were investigated by FTIR spectroscopy and volumetric gas adsorption measurements. The CS$_2$ molecules are η' bonded to Ru sites through one of the sulfur atoms and decompose to the constituent elements on thermal activation. Each S atom may deactivate 3 to 10 metal sites even at low coverages, the effect being more pronounced on the chemisorption of hydrogen. The deposited sulfur (and possibly carbon also) sterically hinders the formation of certain multicarbonyl and monocarbonyl species (νCO in 2055–2140 cm^{-1} region), which otherwise transform to methane via surface methylene groups in the presence of chemisorbed hydrogen and are found to play an important role in the low-temperature methanation activity of the studied catalyst. The Ru–CO species giving rise to lower-frequency vibrational bands are affected to a lesser extent. The presence of sulfur also results in the development of some new CO binding states which are weak and are identified with the CO and S coadsorbed at Ru sites of different oxidation states or of varying crystallographic nature. The CO adsorbed in these states is not reactive to hydrogen. © 1996 Academic Press, Inc.

INTRODUCTION

The trace amount of sulfur in reacting streams is known to poison Group VIII metal catalysts for different adsorption/hydrogenation reactions (1–5) even though some relatively S-resistant noble metal catalysts have also been reported (6). Various issues, such as the mode of adsorption of a sulfur compound on the catalyst surface or its support and the role it plays in the catalytic poisoning, are, however, not yet well resolved. As compared to the studies reported on Ni and Pt metals, only scarce literature is presently available on the S poisoning of Ru metal, particularly when dispersed on an oxide support. We have reported earlier (7) that the exposure of a partially oxidized Ru/TiO$_2$ catalyst to a flow of CO or CO + H$_2$ gave rise to several CO binding states involving ruthenium sites of different oxidation states. These species were identified with the CO held in various multicarbonyl and linear-bonded monocarbonyl forms. With a rise in the catalyst temperature, the multicarbonyl species transformed progressively to monocarbonyls and at temperatures above 420 K, the formation of methylene group-containing hydrocarbon chains was observed. The methylene groups gave way to methane formation when the catalyst temperature was raised further. It was therefore of interest to learn how these individual steps would be affected by the presence of a sulfur compound such as CS$_2$ in the reacting stream. The present Fourier-transform infrared spectroscopic study was carried out to investigate the nature of surface species formed during exposure of a Ru/TiO$_2$ catalyst to the doses of CS$_2$ and then to CO + H$_2$ at different temperatures under static mode conditions. The effect of evacuation in between two exposures and the effect of preadsorbed CO + H$_2$ on the subsequent adsorption of CS$_2$ molecules were also evaluated. Corresponding experiments were performed using metal-free titania to assess the possible role of support in the catalyst poisoning. The effect of preadsorbed sulfur on the H$_2$ and CO adsorption over Ru/TiO$_2$ was evaluated by volumetric methods.

EXPERIMENTAL

Catalyst. The preparation method and the characteristics of a Ru–RuO$_x$/TiO$_2$ catalyst used in this study have been reported earlier (8–10). The catalyst contained about 3.8 wt% of ruthenium with a metal dispersion of about 55% and had a N$_2$ absorption BET area of about 50 m^2 g^{-1}. About 25% of ruthenium existed in the oxide form and the metal particle size ranged between 10 and 30 Å.

FTIR spectroscopy. The infrared spectra were recorded in transmittance mode using a high-pressure, high-temperature stainless-steel cell described earlier in detail (7). The cell had a provision of heating a catalyst wafer *in*

situ at temperatures up to 625 K either under vacuum or in the presence of a desired gas stream. For evacuation, the cell was connected through narrow stainless-steel tubing to a vacuum system equipped with a molecular sieve trap at 77 K and giving a dynamic vacuum of 10^{-5} Torr. The static vacuum achieved in the cell was better than 10^{-3} Torr. The cell used CaF_2 windows mounted on water cooled flanges and the path length was about 6 cm. The catalyst was used in the form of a 25-mm-diameter wafer weighing about 70 mg. Before exposure at a particular temperature and pressure, the catalyst wafer was pretreated under H_2 (500 K, 2 h) and then under vacuum (575 K, 2 h).

A Mattson (USA) model Cygnus-100 FTIR spectrometer using a DTGS detector was employed and 300–400 scans were recorded at 4 cm^{-1} resolution to obtain each spectrum. The IR spectrum of a catalyst wafer recorded after the above-mentioned pretreatments but before admitting adsorbates into IR cell was used as a reference. For the experiments performed at elevated temperatures, the reference spectrum was also obtained under identical conditions. The overlapping bands were computationally resolved using a Fourier self-deconvolution program in the spectrometer software. This was accomplished with the help of the following parameters: full-width at half-maximum (w), enhancement factor (k), fraction Lorentzian (f), and the apodization or smoothing function (a). The value of w (~25 cm^{-1}) was taken directly from one of the well-resolved bands in the undeconvoluted spectrum. The k-factor controlled the amount of resolution enhancement and a value of $k = 1.2$ was found suitable to achieve an optimum S/N ratio. The higher values of k resulted in the large noise signals in deconvoluted spectra. The functions f and a were chosen by trials so that the band shape remained unchanged after deconvolution.

Volumetric measurements. The volumetric adsorption measurements were performed on 200 mg of a sample using a conventional glass vacuum apparatus to evaluate the CO and H_2 uptakes by a catalyst prior to and after its exposure to CS_2 vapor. The irreversibly adsorbed amount of gases was determined by the standard double-isotherm method. Before introducing an adsorbate, the sample was subjected to several cycles of *in situ* treatments under oxygen (400 Torr, 520 K, 30 min) and then under hydrogen (400 Torr, 520 K, 30 min) with 30 min in between evacuation at 10^{-3} Torr. The sample was then degassed at 575 K under vacuum of 10^{-3} Torr for 16 h followed by 3 h evacuation at 10^{-6} Torr.

RESULTS

Effect of Preadsorbed Sulfur on CO and H₂ Adsorption

Figure 1 shows H_2 and CO uptakes on the partially oxidized Ru/TiO_2 catalyst before and after its exposure to various doses of CS_2 vapor at room temperature. The amounts of irreversibly adsorbed CO and H_2 were calculated from the difference between total uptake and that after evacuation at the adsorption temperature for 15 min. A fresh batch of catalyst sample was employed for each experiment with a particular dose of CS_2 vapor. The H_2 and CO uptakes given in Fig. 1 were evaluated for 100 Torr exposure pressure of these gases each time which
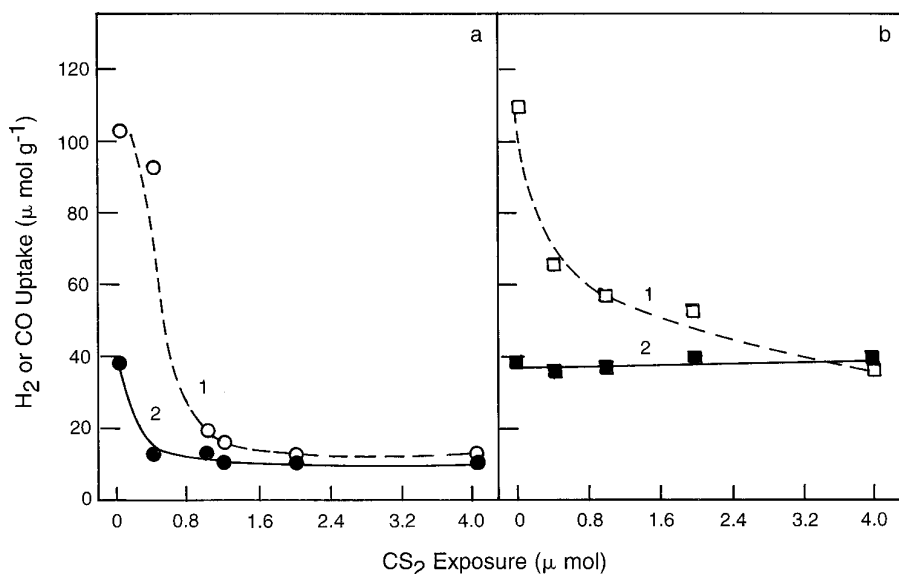

FIG. 1. Effect of CS_2 exposure doses on the H_2 (a) and CO (b) adsorption over Ru/TiO_2 catalyst. Curves 1 and 2 show the irreversible and reversible amounts of adsorbed gases respectively.
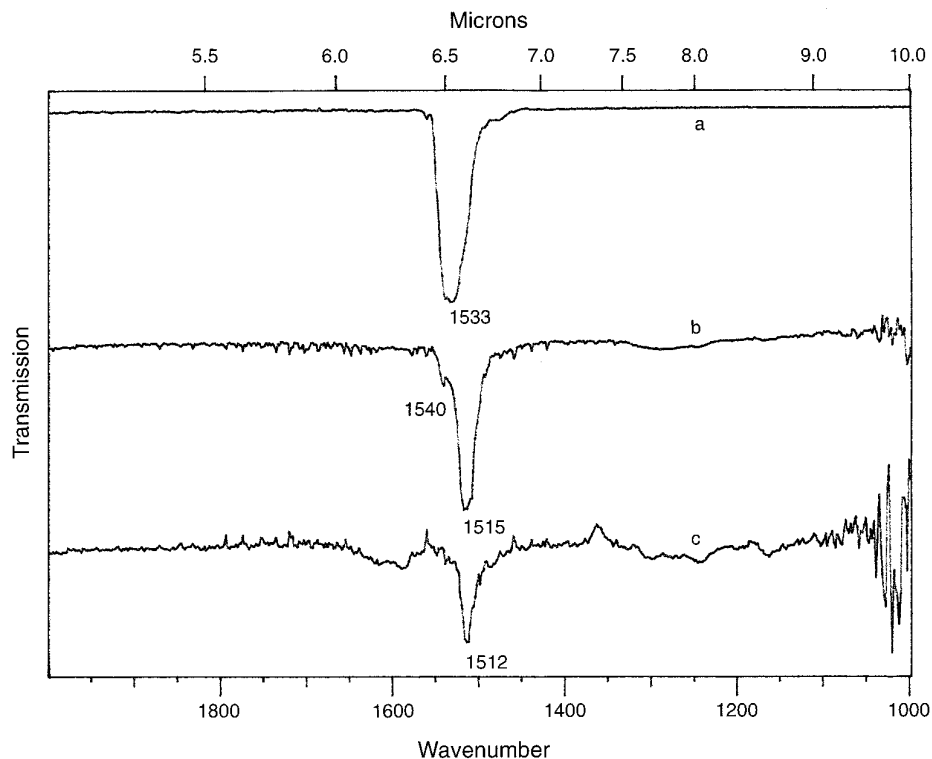
FIG. 2.   IR spectra of (a) gaseous CS$_2$ + H$_e$ (2.4 Torr, 5 μmol CS$_2$) and (b) CS$_2$ adsorbed over Ru/TiO$_2$ at room temperature. (c) Spectrum b after subsequent 20 min evacuation.

was optimized from the independent pressure vs uptake isotherm studies on a fresh lot of sample. The data in Figs. 1a and 1b show that whereas almost similar amounts of CO or H$_2$ were chemisorbed over fresh Ru/TiO$_2$, the amount of adsorbed CO is about four times larger than that of H$_2$ after complete poisoning of the catalyst. These data thus suggest that the presence of CS$_2$ vapor suppressed H$_2$ chemisorption more severely than that of CO.

Infrared spectra of CS$_2$ adsorption.   Spectra a and b of Fig. 2 show vibrational bands when 2.4 Torr of gaseous CS$_2$ + He ($\sim$5 μmol CS$_2$) was introduced into the IR cell without and in the presence of a catalyst wafer. The broadband at 1533 cm^{-1} as seen in Fig. 2a is commensurate with the reported ν(CS$_2$) of free carbon disulfide gas (11). On the exposure over the catalyst surface, the intensity of the 1533 cm^{-1} band decreased sharply and an intense band at 1516 cm^{-1} was observed (Fig. 2b). The intensity of the 1516 cm^{-1} band was reduced on evacuation of the sample as shown in Fig. 1c. This band was removed further on subsequent heat treatment of the sample and disappeared completely at temperatures above 400 K.

IR spectra of Ru/TiO$_2$ on CO + H$_2$ adsorption.   Figure 3 presents the vibrational spectra of a Ru/TiO$_2$ wafer recorded 30 min after exposure to a dose of 100 Torr of CO + H$_2$ (1 : 3) at different temperatures. Various overlap-

ping bands in the C–O stretch region, e.g., at around 2185, 2137, 2080, 2055, 2025, and 2000 cm^{-1}, could be identified in these spectra after a deconvolution (7) in addition to the weak bands at 1614 and 1332 cm^{-1} due to oxygenated species. The frequency of various bands was normally reproducible within ± 2 cm^{-1} when the experiments were repeated with different batches of a sample. In some of the room-temperature CO + H$_2$ exposures, small bands at 2358 and 2340 cm^{-1} due to adsorbed CO$_2$ were also observed. At sample temperatures in the 350–420 K range, a new pair of bands with maxima at around 2926 and 2857 cm^{-1} due to methylene groups was detected, the intensity of which increased with the exposure temperature. Spectra b and c of Fig. 3 illustrate these bands for the exposure temperatures of 370 and 420 K. Further increase in the sample temperature resulted in the removal of 2926 and 2857 cm^{-1} bands and gave rise to the formation of two new bands at 3017 and 1305 cm^{-1} due to methane. The complete conversion of CO + H$_2$ to methane gas was observed at the sample temperatures above 450 K (Fig. 3d). As shown in spectra a–d of Fig. 3, the temperature-dependent formation of methylene groups and methane was accompanied with the progressive removal of higher frequency C–O stretch bands in the 2185–2050 cm^{-1} region whereas the vibrational bands appearing at the lower frequencies ($<$2050 cm^{-1}) remained almost unchanged. It can
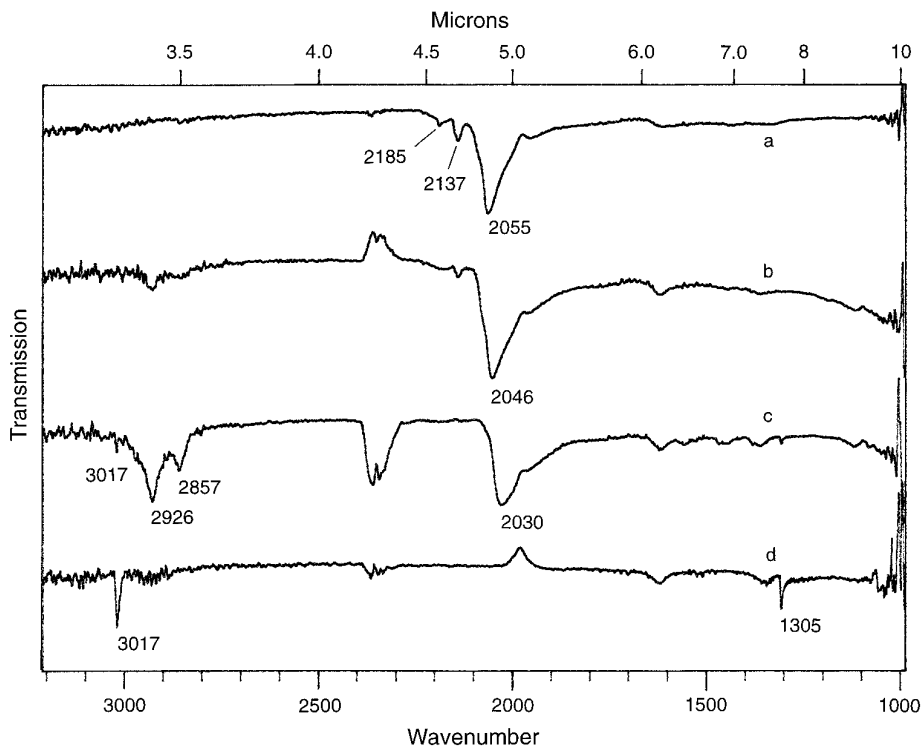
FIG. 3. IR spectra of Ru/TiO$_2$ following 30 min exposure to 100 Torr CO + H$_2$ (1:4) at (a) room temperature (b) 370 K, (c) 420 K, and (d) 470 K.

therefore be concluded that the species responsible for higher frequency vibrational bands are the source of methane at reaction temperatures below 475 K as has also been discussed before (7).

The results shown in Fig. 3 are similar to the data reported in Ref. (7) for the experiments performed under continuous flow of CO + H$_2$. The time- and the temperature-dependent growth of C–O stretch bands developed on Ru/TiO$_2$ catalyst under static conditions was also similar to those described earlier (7) in detail.

Effect of Preadsorbed Sulfur on IR Spectra of CO + H$_2$ Adsorption

Figure 4a gives the vibrational spectrum of a Ru/TiO$_2$ wafer exposed to 2.4 Torr of CS$_2$ + He (5 μmol CS$_2$) followed immediately by the introduction of 100 Torr CO + H$_2$ (1:4) at ambient temperature. The 1516 cm^{-1} band in this figure corresponds to the adsorbed CS$_2$ as shown in Fig. 2. Spectra b and c in this figure show IR bands obtained after raising the sample temperature to 370 and 470 K, respectively. No methylene group chains or methane was formed in this case in contrast to the data obtained on a S-free catalyst surface (Fig. 3). No gaseous CS$_2$ was released during subsequent thermal treatment indicating complete dissociation of adsorbed CS$_2$.

A better picture of the sulfur effect on the C–O stretch bands is presented in Fig. 5, which shows wide-range spectra obtained on subtracting IR bands due to gaseous CO from the spectra in Fig. 4. For this purpose CO + H$_2$ were admitted over metal-free titania at different pressures and difference spectra were then obtained using IR bands of matching intensities. Spectra a–c in Fig. 5 show these difference spectra corresponding to C–O stretch bands in Figs. 4a–4c after having been deconvoluted using parameters of $w = 25$, $k = 1.2$, $f = 0.4$, and $a = 3$ for better discernation of individual vibrational bands. A comparison with the similar results obtained on a S-free catalyst wafer (Ref. (7)) shows that the vibrational bands in the 2050–2140 cm^{-1} region as seen in Fig. 3 are either weak or completely missing in the corresponding spectra in Fig. 5. Instead, new bands at around 2101 and 2013 cm^{-1} are clearly discernable in the spectra of Fig. 5, indicating the formation of new surface species.

When the IR cell was evacuated between the CS$_2$ + He exposure and the introduction of 100 Torr CO + H$_2$ as mentioned above, the spectra as shown in Figs. 6a–6d were obtained at different catalyst temperatures. Again, no methylene groups or methane was formed at sample temperatures up to 470 K (cf. Fig. 3). It may also be noted that the 2013 cm^{-1} band in Fig. 5 now appears at a new

frequency of 2034 cm^{-1}. The frequency of this band shifted to a lower value on a rise in the sample temperature (Figs. 6c and 6d) even though its intensity remained unchanged.

Intercomparison of C–O Stretch Bands

To enable us to make a better comparison of the individual component bands in the C–O stretch region, spectra a–c in Fig. 7 present deconvoluted spectra corresponding to C–O stretch region bands in Figs. 3a, 4a, and 6a. It may be mentioned that as in the case of Fig. 5, the spectra in Fig. 7 were obtained after subtracting gas-phase vibrational bands from the respective data of Figs. 3, 4, and 6. Spectra a and b in Fig. 7 show that the S coverage results in the reduced intensity of the bands appearing at 2141, 2085, and 2055 cm^{-1}. On the other hand, new bands at 2104–2109, 2033, and 2011 cm^{-1} were observed in the case of S-covered samples. Of these, the 2033 cm^{-1} band was observed on a surface exposed to CS$_2$ followed by evacuation (Fig. 6). Since almost all the bands observed on a S-free catalyst (Fig. 7a) existed simultaneously in the spectra b and c of this figure, although with reduced intensities, and since our experiments were performed at a constant CO + H$_2$ pressure of 100 Torr, it may be inferred that the new bands mentioned above are not due to frequency shifts attributable to dipole–dipole interactions arising because of surface coverage effects.

Effect of CS$_2$ Dose

When a smaller amount of CS$_2$ (∼0.5 μmol) was dosed over the catalyst wafer, weak bands at 2855 and 2927 cm^{-1} due to methylene groups were observed during subsequent catalyst exposure to CO + H$_2$ at temperatures in the 400–475 K region (cf. Fig. 3c). No CH$_4$ was, however, formed at any stage. The intensity of νCH$_2$ bands decreased further with increasing amounts of preadsorbed CS$_2$ and no such bands were formed for CS$_2$ doses of more than 1 μmol.

CS$_2$ Adsorption over CO-Covered Ru/TiO$_2$

When the sequence of CO and CS$_2$ interaction was changed, i.e., a catalyst wafer was first exposed to 100 Torr of CO + H$_2$ (1:4) and then to CS$_2$ vapor, the IR bands due to adsorbed CO remained unaltered both in terms of their intensity and their frequency. Spectra a and b of Fig. 8 were obtained when a Ru/TiO$_2$ wafer exposed to 100 Torr CO + H$_2$ at ambient temperature was further dosed with 0.5 and 6 μmol of CS$_2$ (in helium), respectively. For comparison, spectrum c in this figure shows vibrational bands developed over Ru/TiO$_2$ on 100 Torr CO + H$_2$ (1:4) exposure at room temperature. As seen in this figure, the νCO band at 2058 cm^{-1} observed on S-free catalyst (Fig. 8c) is observed at 2056 cm^{-1} even when the catalyst was exposed further to ∼3 Torr CS$_2$ + He (∼6 μmol CS$_2$).
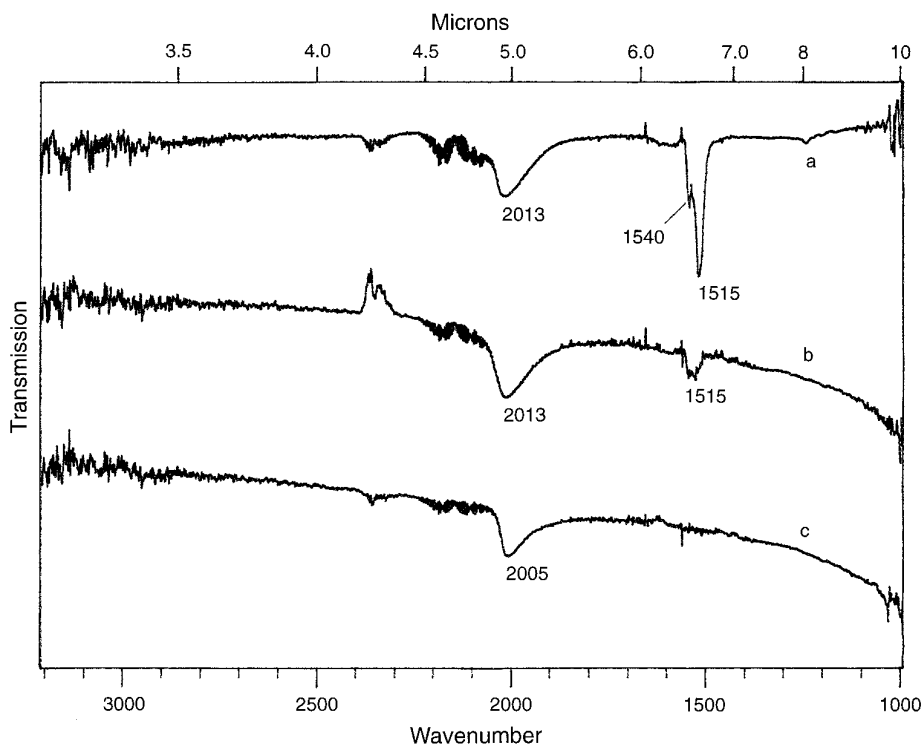

FIG. 4. IR spectra of Ru/TiO$_2$ exposed to 2.4 Torr of CS$_2$ + H$_e$ (5 μmol CS$_2$) followed by introduction of 100 Torr CO + H$_2$ (1:4) at ambient temperature (spectrum a). Spectra b and c show IR bands obtained on subsequent rise in sample temperature to 370 and 470 K respectively.
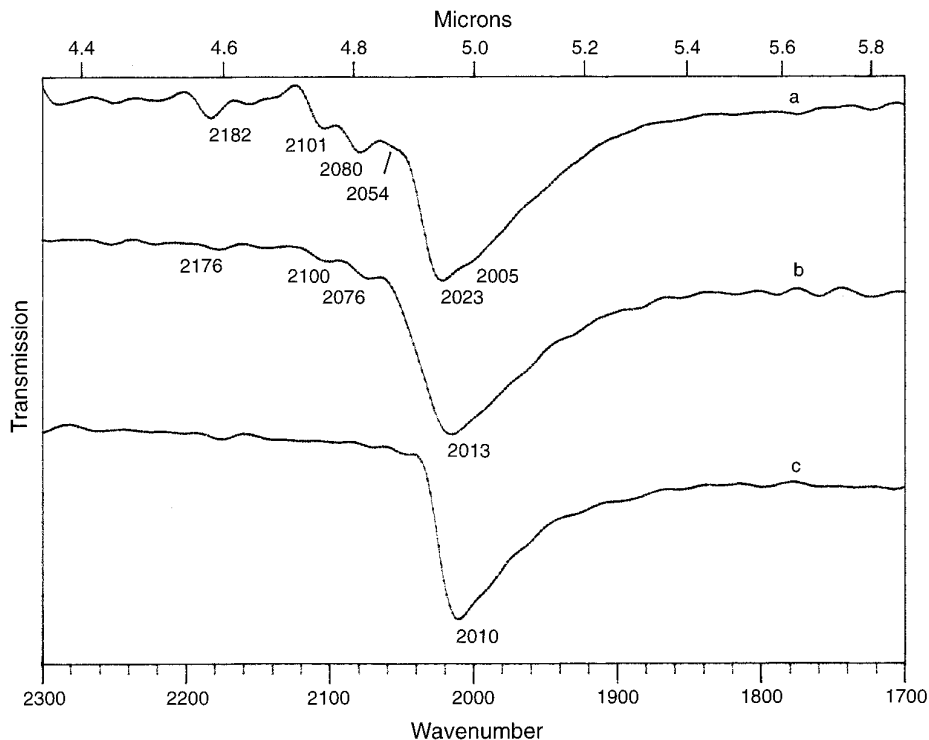
FIG. 5. Spectra a–c show difference C–O stretch region spectra corresponding to Figs. 4a–4c obtained on subtracting IR bands due to gaseous CO in the IR cell and after deconvolution using parameters: $w = 25$, $k = 1.2$, $f = 0.4$, and $a = 3$.
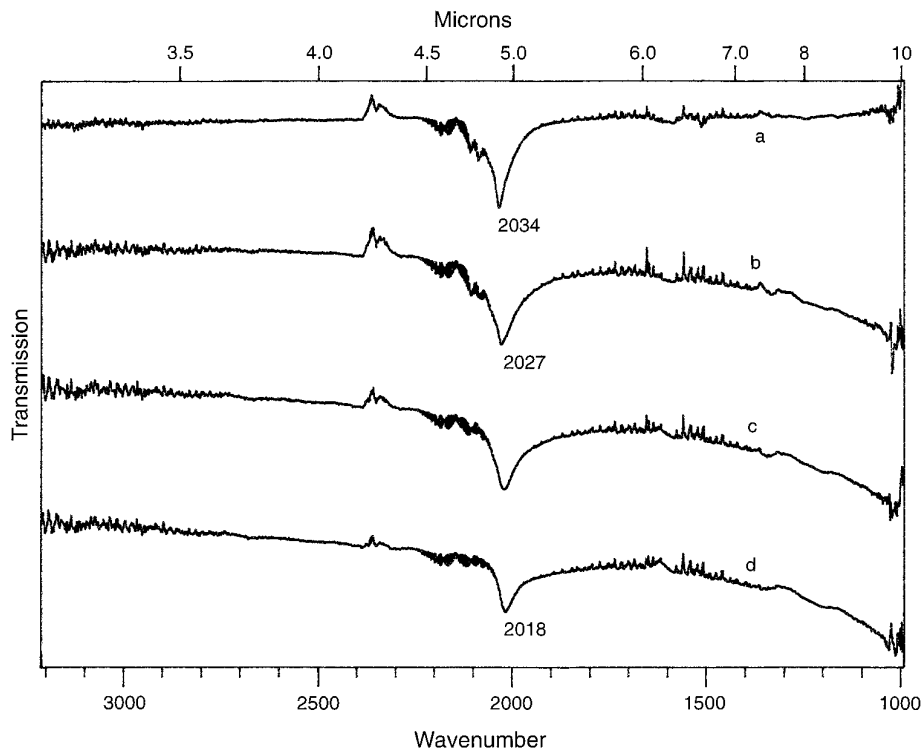

FIG. 6. IR spectra of Ru/TiO$_2$ exposed to 2.4 Torr of CS$_2$ + H$_e$ (5 μmol CS$_2$) followed by evacuation (10^{-3} Torr) and then introduction of 100 Torr CO + H$_2$ (1 : 4) at ambient temperature (spectrum a). Spectra b–d show the effect of raising sample temperature to 370, 420, and 470 K respectively.

It is also of interest to observe that some amount of CS$_2$ is still adsorbed (1516 cm^{-1} band) on a catalyst surface which is already saturated with adsorbed CO (Fig. 8b).

CS$_2$ Adsorption over Ru-Free Titania

νCS$_2$ bands similar to those observed on adsorption of CS$_2$ over Ru/TiO$_2$ (Fig. 2) were also formed when a metal-free titania sample was exposed to CS$_2$ (Fig. 9a). The CS$_2$ was, however, adsorbed weakly and was removed completely when the IR cell was pumped for a few minutes. Figure 9b shows a typical spectrum of TiO$_2$ wafer exposed to 5 μmol CS$_2$ followed by a 2-min evacuation. No gaseous CS$_2$ was released and the 1516 cm^{-1} band disappeared when the sample was heated subsequently to 420 K.

DISCUSSION

Carbon disulfide is known to bind a metal atom in different modes I–VI shown below (12, 13) and each mode of bonding can readily be identified by C–S stretchings in the infrared spectra (11).

(I)   (II)   (III)

(IV)   (V)   (VI)
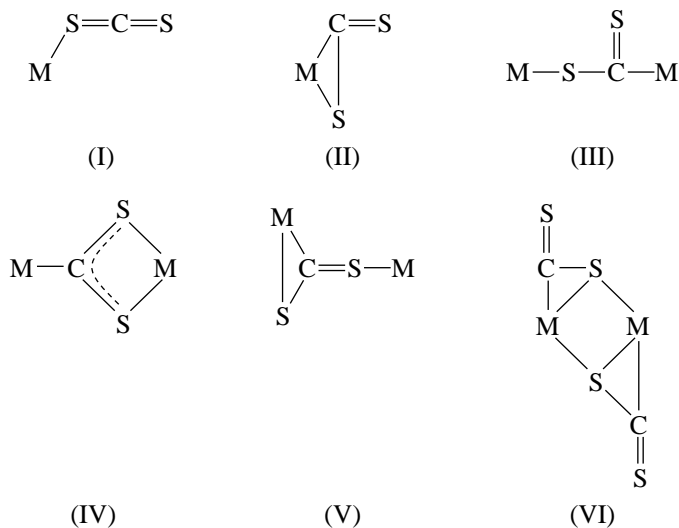
Excepting end-on-S-bonded η^1 complexes (I) (νCS ~1510 cm^{-1}), other CS$_2$ complexes have either the three-membered η^2-type (II) (νCS, 1100–1160 cm^{-1}) or bridging (III–VI) (νCS 840–1120 cm^{-1}) structures (11–16). The vibrational spectrum in Fig. 2b thus shows that the CS$_2$ is bonded to Ru/TiO$_2$ catalyst in η^1 (end-on-S-bonding) mode (structure I). The bonding is fairly strong as the adsorbed CS$_2$ is only partly removed on evacuation (Fig. 2c). Furthermore, no molecular CS$_2$ was desorbed on subsequent heating of the sample indicating its complete dissociation. The dissociation of CS$_2$ may result in the formation of some thiocarbonyl (CS) complexes on the catalyst, such as shown below:

(VII)   (VIII)   (IX)
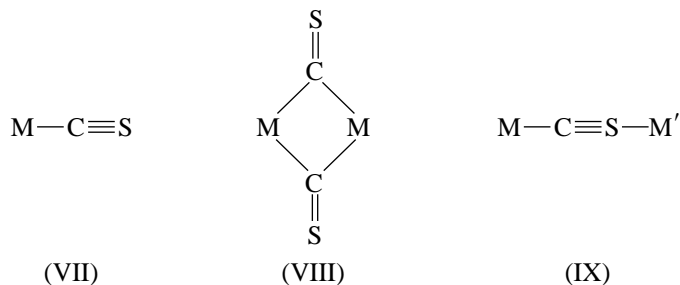
As reviewed in (11), while the ν(CS) of free CS is observed at 1275 cm^{-1} the C-bonded terminal CS groups give a vibrational band at a higher frequency in the region 1290–1360 cm^{-1}. The bridging C-bonded structure VIII is assigned ν(CS) at ~1125 cm^{-1} (17). The vibrational spectra obtained in the present study (Figs. 2–4) thus show that no significant number of carbon-bonded species shown above are formed during adsorption and dissociation of CS$_2$ over Ru/TiO$_2$ without or in the presence of CO. Figure 9 shows that CS$_2$ is adsorbed on metal-free titania also even though the bonding is weak and the CS$_2$ is almost completely removed on subsequent evacuation. No bands due to free carbon disulfide were observed, however, when a titania sample exposed to CS$_2$ was heated subsequently (Fig. 9c) indicating that the CS$_2$ is decomposed even in the absence of Ru metal. Two weak bands at ca. 1180 and 1250 cm^{-1} in Figs. 9a and 9b suggest the presence of a small number of surface species such as those shown in the structures VI and VII above.

Effect of S on C–O Stretch Bands

The frequencies of C–O stretch bands are known to depend upon various factors, such as the nature, dispersion, oxidation state, and crystallographic phase of the exposed metal in addition to the nature of support, surface coverage, and the reaction condition (18–33). The chemisorption of CO on supported Ru is reported to give at least three vibrational bands (at around 2140, 2080, and 1990–2030 cm^{-1}). The band at around 2000 cm^{-1} is generally attributed to CO bonded linearly to Ru, although discrepant views have been expressed about the origin of higher-frequency bands. For example, in an early study of Brown and Gonzalez (21), the bands observed at 2135 and 2080 cm^{-1} were assigned to the CO-stretching vibration of CO adsorbed on a surface oxide and CO adsorbed on a Ru atom perturbed by a nearby oxygen atom respectively. In the later studies by Robbins (29) and Chen et al. (26) using isotopically labeled CO, the 2140 and 2085 cm^{-1} bands were found to be the coupled vibrations of an Ru(CO)$_x$ (x = 2 or 3) species and this assignment is now widely accepted (22–25, 30–32). A band at around 2132–2136 cm^{-1} in conjunction with the 2085 cm^{-1} band is similarly assigned to a multicarbonyl species bonded to Ru in a higher oxidation state
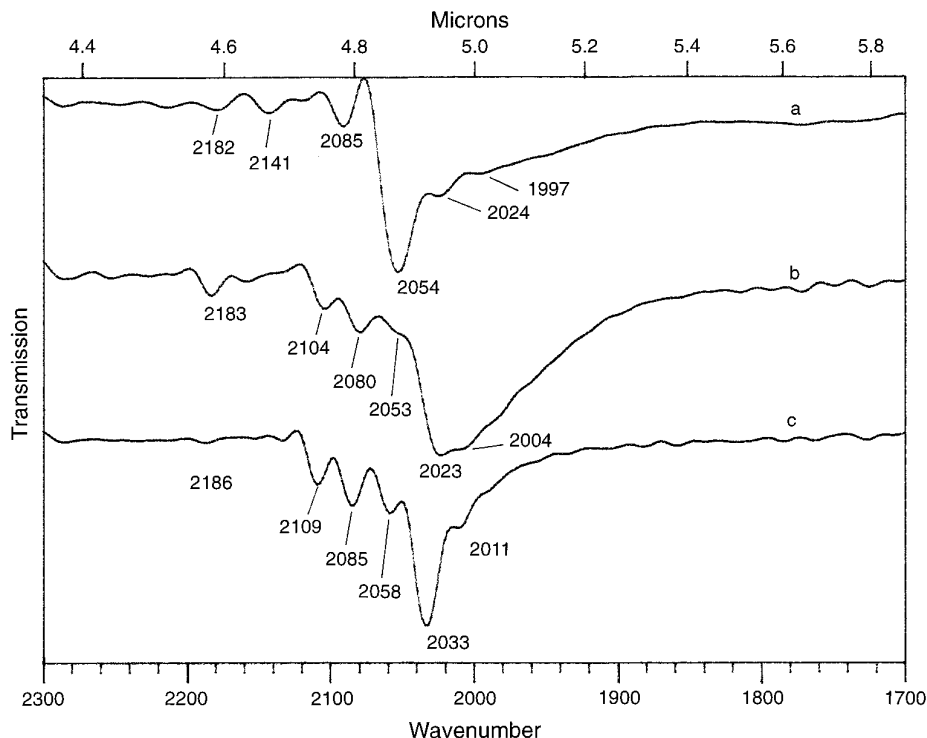
FIG. 7. Deconvoluted C–O stretch region spectra of Ru/TiO$_2$ (a) exposed for 30 min to CO + H$_2$ (1:4) at 300 K, (b) exposed to 2.4 Torr of CS$_2$ + H$_e$ followed by 100 Torr of CO + H$_2$ (1:4) at 300 K, (c) exposed to 2.4 Torr CS$_2$ + H$_e$ followed by evacuation and dosing of 100 Torr CO + H$_2$ (1:4) at 300 K.

(18, 31, 32). A study in our laboratory has shown the development of at least six vibrational bands in the 1950–2142 cm^{-1} region during adsorption of CO over partially oxidized Ru on titania catalyst (7) and based on the discussion given above and also in our earlier publications (7, 18, 19), the possible assignments of vibrational bands shown in Figs. 3–8 are given in Table 1. We thus assign the νCO bands at 2141 and 2085 cm^{-1} in Fig. 7 to multicarbonyl species, whereas the vibrational bands appearing at 2054, 2024, and 1997 cm^{-1} may be ascribed to monocarbonyls bonded linearly at ruthenium sites of different oxidation states or of varying crystallographic/morphological nature (shown as Ru and Ru′ sites in Table 1).

Various theories have been put forward to explain the influence of sulfur on the adsorptive and the catalytic properties of metal surfaces, such as the electronic effects involving short-range or long-range surface–adsorbate interactions, geometric effects involving site blocking, and the reconstruction or surface morphology changes, even though much of this work is confined to single-crystal surfaces. For example, van Santen (27) showed that the coadsorbed sulfur induces changes in the electronic structure of the transition metals as a result of which the CO adsorbed on a metal atom whose nearest neighbor metal atom is coordinated with S could be more strongly bonded.

Similarly, Goodman and Kiskinova (34, 35) explained the reduction in CO saturation coverage by preadsorbed sulfur on the basis of long-range interactions. On the other hand, Apesteguia *et al.* (36) showed that the predeposited S on Pt caused an upward shift of ν(CO) from 2068 to 2083 cm^{-1}. This effect was explained by a localized modification of the metal by the electron-acceptor properties of irreversibly held sulfur. Padley *et al.* (37) recently reported both site-blocking and electronic effects of thiophene on CO adsorption over Cu/Al$_2$O$_3$ catalyst. Various authors have shown the development of new CO-binding states on S-covered transition metals (38–41). In this state CO is considered to be bonded very weakly to single-metal atoms. Thermal desorption spectroscopy studies of Garfunkel *et al.* (42) have similarly demonstrated that the coadsorbed sulfur resulted in the weakening of CO bonding over Pt(111) surface.

The spectra in Figs. 3–6 and the deconvoluted bands in Fig. 7 clearly show that the various vibrational bands seen on CO adsorption on a fresh catalyst coexist, although with diminished intensity, with the new bands at around 2104, 2034, and 2011 cm^{-1} observed on S-covered surfaces (Figs. 5, 6). These observations thus indicate that on one hand the presence of sulfur inhibits the formation of certain multicarbonyl species (Ru(CO)$_x$, νCO 2141/2137, 2085
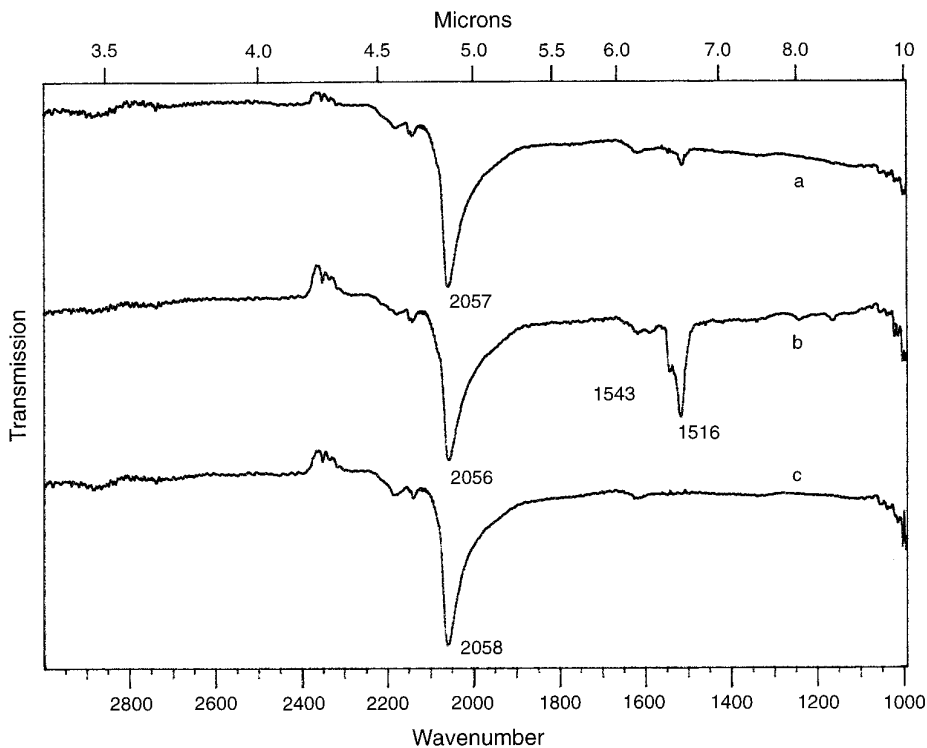
FIG. 8. IR spectra of Ru/TiO$_2$ when exposed at room temperature to 100 Torr CO + H$_2$ (1:4) followed by dosing of 0.5 (spectrum a) and 6 (spectrum b) μmol of CS$_2$ (in helium). Spectrum c shows comparative vibrational bands developed on Ru/TiO$_2$ on CO + H$_2$ (1:4) adsorption.
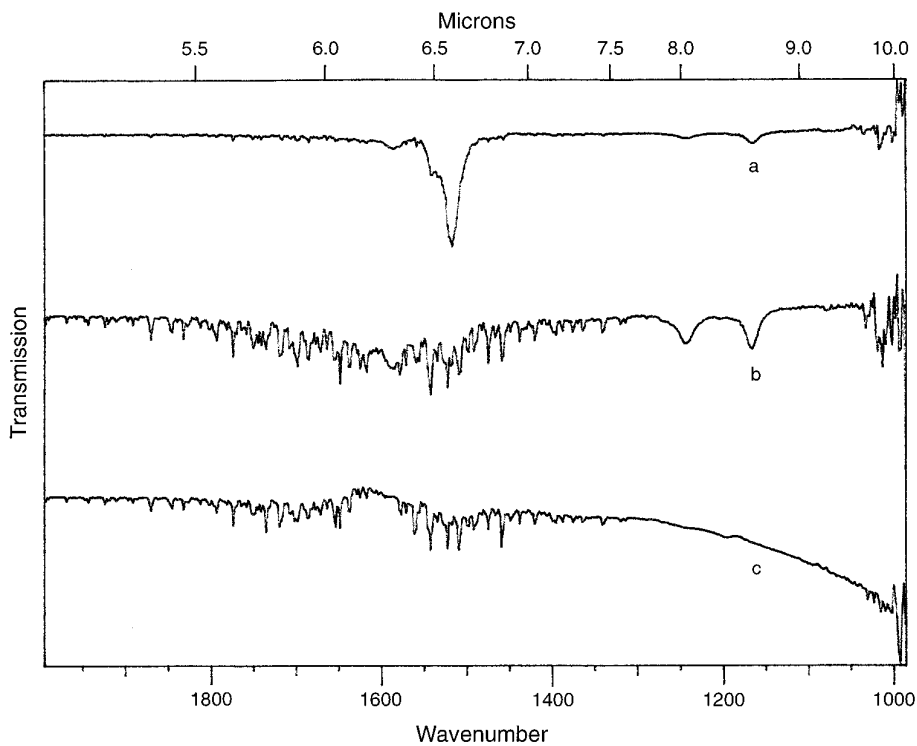

FIG. 9. IR spectra of metal free TiO$_2$ exposed for 30 min to 2.4 Torr CS$_2$ + H$_e$ at 300 K (spectrum a) and evacuated subsequently for 2 min (spectrum b). (c) Spectrum a after raising sample temperature to 420 K.

TABLE 1

C–O Stretch Bands Observed during Room Temperature Adsorption of CO + H₂ over Fresh and S-Covered Ru–RuO$_x$/ TiO₂ Catalyst (Fig. 7)

Frequency	Assignment	Effect of preadsorbed sulphur
2182–2185	Physisorbed CO	No effect
2141/2136	Ru(CO)$_n$/RuO$_x$(CO)$_n$	Diminished
2104–2109	Ru$\overset{\diagup S}{\diagdown CO}$	New species
2080–2085	Ru(CO)$_n$ + RuO$_x$(CO)$_n$	Diminished
2053–2058	Ru(CO)	Diminished
2033	Ru$^{\delta+}\overset{\diagup S}{\diagdown CO}$	New species
2023–2025	Ru′O$_x$(CO)	Increases
2011	Ru′$\overset{\diagup CO}{\diagdown S}$	New species
~1960	Ru′–CO	No effect

cm⁻¹) and linearly bonded species (νCO 2055 cm⁻¹), and on the other hand it gives rise to new CO-binding states responsible for the vibrational bands at 2104, 2034, and 2013 cm⁻¹ (Figs. 5, 6). These bands are removed easily at elevated temperatures (Figs. 5, 6) indicating their weak bonding. Also a small difference in the frequency of these bands from those observed on a S-free surface may be attributed to small perturbations due to a weak electronic interaction between the coadsorbed species at a metal site. On the basis of these arguments, we assign the new vibrational bands to surface structures composed of coadsorbed CO and S at Ru sites of different oxidation states or of different crystallographic nature, even though their unequivocal identification is not possible at present. The suggested assignments to these bands are given in Table 1. Since CS₂ decomposed easily on the catalyst surface (Figs. 2, 4), it is likely that the deposited carbon may also alter CO-binding states depending upon the catalyst temperature.

Data in Fig. 8 show that the CS₂ molecules do not displace CO molecules held already at Ru sites at room temperature. These results therefore indicate that under this condition both the CS₂ and CO molecules compete for Ru sites and the presence of one adsorbate at a metal site causes hindrance to adsorption of the other. A similar situation may be envisaged at the higher reaction temperatures when both the CO and CS₂ are likely to decompose and block the surface sites.

Effect of Sulfur on CO and H₂ Chemisorption

Almost similar amounts of CO and H₂ (~40 μmol g⁻¹) held reversibly over a fresh catalyst may be associated with these gases adsorbed over support (Figs. 1a, 1b). The data in Fig. 1 also show that an almost similar number of CO and H₂ molecules were irreversibly adsorbed over S-free catalyst surface. If the irreversible adsorption stoichiometry for hydrogen is taken as 1 H$_{(ad)}$ per surface Ru (Ru$_s$), then two metal sites would be involved for the adsorption of one hydrogen molecule. As no formation of bridge-bonded CO species is indicated in our infrared data, the ratio of metal sites associated with chemisorption of H₂ and CO molecules may thus be considered as 2:1. The chemisorption data therefore confirm the formation of certain Ru(CO)$_x$ species shown in Table 1. Data in Fig. 1 also show that very small CS₂ amount is capable of poisoning the catalyst surface, the chemisorption of H₂ being more drastically reduced (Fig. 1a) as compared to that of CO (Fig. 1b). Thus, for the 41-μmol Ru$_s$ sites available in the used amount of catalyst, while almost all the metal sites were involved in H₂ chemisorption, only about 60% of the sites were occupied by CO under saturation coverage conditions (Fig. 1). An exposure to ~1.5-μmol CS₂ (CS₂/ Ru$_S$ ratio = 0.036 assuming adsorption occurs on the Ru only) decreases irreversible H₂ adsorption by 8-fold to about 15 μmol g⁻¹ and that of CO by 2.5-fold to about 45 μmol g⁻¹. The observation that about 20% of the total Ru$_s$ sites were still available for CO chemisorption at a stage when the hydrogen chemisorption was almost completely suppressed (Fig. 1) is in agreement with our infrared results of Figs. 4 and 5 which show that the higher frequency νCO bands are preferentially affected by S coverage leaving behind some unperturbed metal sites. The nonreactivity of these residual CO$_{(ad)}$ species (Fig. 6) for methanation reaction may thus be attributed to the nonavailability of much needed chemisorbed hydrogen.

Our results are in agreement with the single-crystal studies of Goodman and Kiskinova (34, 35) who reported that the poisoning effect of sulfur is nonlinear and one sulfur atom deactivates approximately 8–10 nickel atom sites. Jorgensen and Madix (43) showed that ~0.1 monolayer of sulfur coverage resulted in the rapid decrease in the CO saturation coverage over the Pd(100) surface and the effect is attributed to disorder in the CO adlayer induced by the preadsorbed sulfur. It was suggested that at low coverages, the immobile sulfur atoms cause local CO–S interaction, which in turn prevents the phase transition of CO from the c(2 × 2) to a high-density compression structure. At increased sulfur coverages, the poisoning was found to proceed by site blockings only. Brand *et al.* (44) similarly demonstrated that the hydrogen mobility decreases rapidly with the S coverage on Ru(001) surface. It was shown that one sulfur atom blocked 10 hydrogen adsorption sites and

the effect of sulfur was attributed to both the steric and the long-range electronic effects. Carbon was similarly found to reduce significantly the mobility of hydrogen on Ru(001) (45).

SUMMARY

The results discussed above help us in arriving at the following conclusions: Sulfur poisoning behavior of supported Ru bears similarity with the reported S-coverage effects on the CO chemisorption over Group VIII metal single crystals. Both the CO and CS$_2$ compete for those Ru sites which are responsible for CO adsorption and its subsequent hydrogenation. The CS$_2$ molecules are η^1 bonded to Ru sites through one of the sulfur atoms. This bonding is fairly strong and the adsorbed CS$_2$ decomposes to the constituent elements on thermal activation. Even a small amount of sulfur (S/Ru$_s$ $\sim$0.05) is effective in poisoning the catalytic activity of Ru and each S atom may deactivate 3 to 10 metal sites. The sulfur coverage effect was more pronounced on the chemisorption of hydrogen. The results indicate that the sulfur and carbon atoms sterically hinder the formation of certain multicarbonyl and monocarbonyl surface species which otherwise transform to methylene groups and then to methane in the presence of hydrogen and are found to play an important role in the low-temperature methanation activity of the catalyst under study (7, 18). Considering that the dispersed metal exists in form of ensembles of varying sizes over catalyst surface, it is suggested that the closely packed CO$_{(ad)}$ or H$_{(ad)}$ states bound together by weak electronic forces exist at such ensembles and the number of molecules held at a site depends on the ensemble size. The perturbation of one metal atom by S coverage may therefore influence various neighboring ad-states, thus explaining why one sulfur atom inhibits adsorption of more than one gas molecule, as mentioned above. This explanation is in line with the proposed concept of CO ''compression'' structures on transition-metal single crystals (43), where small concentrations of surface impurities impede its formation. For low surface coverages, no methane was produced in our study even when methylene species were formed during CO + H$_2$ reaction at temperatures between 370 and 470 K, and this may be correlated to the drastic loss in H$_2$ chemisorption. This also confirms that the chemisorption of both the H$_2$ and CO molecules is vital for CO hydrogenation reaction. The presence of sulfur also results in the development of some new CO-binding states which are identified with the CO and S coadsorbed at Ru sites of different oxidation states or crystallographic nature. CO in these states is held weakly and is not hydrogenated even in the presence of excess hydrogen.

The role of the CS$_2$ adsorbed and decomposed over the titania support in catalytic poisoning is not clear at present.

It is likely that sulfur deposited on the titania support may physically block the transport/adsorption of hydrogen or carbon monoxide at the adjacent Ru sites.

REFERENCES

1. Madon, R. J., and Shaw, H., *Catal. Rev.-Sci. Eng.* **15,** 69 (1977).
2. Oudar, J., *Catal Rev.-Sci. Eng.* **22,** 171 (1980).
3. Hegedus, L. L., and McCabe, R. W., *Catal. Rev.-Sci. Eng.* **23,** 377 (1981).
4. Bartholomew, C. H., Agrawal, P. K., and Katzer, J. R., *Adv. Catal.* **31,** 135 (1982).
5. Agrawal, P. K., Katzer, J. R., and Manogue, W. H., *J. Catal.* **74,** 332 (1982); **69,** 327 (1981).
6. Berube, M. N., Sung, B., and Vannice, M. A., *Appl. Catal.* **31,** 133 (1987).
7. Gupta, N. M., Kamble, V. S., Iyer, R. M., Thampi, K. R., and Gratzel, M., *J. Catal.* **137,** 473 (1992).
8. Thampi, K. R., Kiwi, J., and Gratzel, M., *Nature* **327,** 506 (1987).
9. Highfield, J. G., Ruterna, P., Thampi, K. R., and Gratzel, M., *in* ''Structure and Reactivity of Surfaces'' (C. Morterra, A. Zecchina, and G. Costa, Eds.), p. 469. Elsevier, Amsterdam, 1989.
10. Thampi, K. R., Lucarelli, L., and Kiwi, J., *Langmuir* **7,** 2642 (1991).
11. Nakamoto, K., ''Infrared and Raman Spectra of Inorganic and Coordination Compounds,'' 3rd ed., p. 116. Wiley-Interscience, New York, 1978.
12. Yaneff, P. V., *Coord. Chem. Rev.* **23,** 183 (1977).
13. Butler, I. S., *Acc. Chem. Res.* **10,** 359 (1977).
14. Baird, M. C., Hartwell, G., and Wilkinson, G., *J. Chem. Soc. A,* 2037 (1967).
15. Baird, M. C., and Wilkinson, G., *J. Chem. Soc. A,* 865 (1967).
16. Butler, I. S., and Fenster, A. E., *J. Organometal. Chem.* **6,** 161 (1974).
17. Efraty, A., Arneri, R., and Huang, M. H. A., *J. Am. Chem. Soc.* **98,** 639 (1976).
18. Gupta, N. M., Kamble, V. S., Kartha, V. B., Iyer, R. M., Thampi, K. R., and Gratzel, M., *J. Catal.* **146,** 173 (1994).
19. Gupta, N. M., Kamble, V. S., Iyer, R. M., Thampi, K. R., and Gratzel, M., *Catal. Lett.* **21,** 245 (1993).
20. Dalla Betta, R. A., *J. Phys. Chem.* **79,** 2519 (1975).
21. Brown, M. F., and Gonzalez, R. D., *J. Phys. Chem.* **80,** 1731 (1976).
22. Davydov, A. A., and Bell, A. T., *J. Catal.* **49,** 332 (1977).
23. Kunnetsov, V. L., Bell, A. T., and Yermakov, Y. J., *J. Catal.* **65,** 374 (1980).
24. Yamasaki, H., Kobori, Y., Naito, S., Onishi, T., and Tamaru, K., *J. Chem. Soc., Faraday Trans. 1* **77,** 2913 (1981).
25. Guglielminotti, E., Zecchina, A., Bossi, A., and Camia, M., *J. Catal.* **74,** 240 (1982).
26. Chen, H. W., Zhong, Z., and White, J. M., *J. Catal.* **90,** 119 (1984).
27. van Santen, R. A., *J. Chem. Soc., Faraday Trans. 1* **83,** 1915 (1987).
28. Hoffman, F. M., and Robbins, J. L., *in* ''Proceedings, 9th International Congress on Catalysis, Calgary, 1988'' (M. J. Phillips and M. Ternan, Eds.), Vol. 3, p. 1144. Chem. Institute of Canada, Ottawa, 1988.
29. Robbins, J. L., *J. Catal.* **115,** 120 (1989).
30. Solymosi, F., and Raskó, J., *J. Catal.* **115,** 107 (1989).
31. Yokomizo, G. H., Louis, C., and Bell, A. T., *J. Catal.* **120,** 1, 1989.
32. Guglielminotti, E., and Bond, G. C., *J. Chem. Soc., Faraday Trans.* **86,** 979 (1990).
33. Mc Quire, M. W., and Rochester, C. H., *J. Catal.* **141,** 355 (1993).

34. Goodman, D. W., and Kiskinova, M., *Surf. Sci.* **105,** L 265 (1981).
35. Goodman, D. W., and Kiskinova, M., *Surf. Sci.* **108,** 64 (1981).
36. Apesteguia, C. R., Brema, C. E., Garetto, T. F., Borgna, A., and Parera, J. M., *J. Catal.* **89,** 52 (1984).
37. Padley, M. B., Rochester, C. H., Hutchings, G., and King, F., *J. Catal.* **148,** 438 (1994).
38. Wentrcek, P. W., McCarty, J. G., Ablow, C. M., and Wise, H., *J. Catal.* **61,** 232 (1980).
39. Trenary, M., Uram, K. J., and Yates, Jr., J. T., *Surf. Sci.* **157,** 512 (1985).
40. Benziger, J., and Madix, R. J., *Surf. Sci.* **94,** 119 (1980).
41. Gland, J. L., Madix, R. J., McCabe, R. W., and De Maggio, C., *Surf. Sci.* **143,** 46 (1984).
42. Garfunkel, E. L., Farias, M. H., and Somorjai, G. A., *J. Am. Chem. Soc.* **107,** 349 (1985).
43. Jorgensen, S. W., and Madix, R. J., *Surf. Sci.* **163,** 19 (1985).
44. Brand, J. L., Deckert, A. A., and George, S. M., *Surf. Sci.* **194,** 457 (1988).
45. Mak, C. H., Koehler, B. G., Brand, J. L., and George, S. M., *J. Chem. Phys.* **87,** 2340 (1987).